

The Crystal Structure of *Nitrosomonas europaea* Sucrose Synthase Reveals Critical Conformational Changes and Insights into Sucrose Metabolism in Prokaryotes

Rui Wu,^a Matías D. Asención Díez,^{a,b} Carlos M. Figueroa,^{a,b} Matías Machtey,^b Alberto A. Iglesias,^b Miguel A. Ballicora,^a Dali Liu^a

Department of Chemistry and Biochemistry, Loyola University Chicago, Chicago, Illinois, USA^a; Instituto de Agrobiotecnología del Litoral, Universidad Nacional del Litoral and Consejo Nacional de Investigaciones Científicas y Técnicas, Centro Científico Tecnológico Santa Fe, Santa Fe, Argentina^b

ABSTRACT

In this paper we report the first crystal structure of a prokaryotic sucrose synthase from the nonphotosynthetic bacterium *Nitrosomonas europaea*. The obtained structure was in an open form, whereas the only other available structure, from the plant *Ara-bidopsis thaliana*, was in a closed conformation. Comparative structural analysis revealed a “hinge-latch” combination, which is critical to transition between the open and closed forms of the enzyme. The *N. europaea* sucrose synthase shares the same fold as the GT-B family of the retaining glycosyltransferases. In addition, a triad of conserved homologous catalytic residues in the family was shown to be functionally critical in the *N. europaea* sucrose synthase (Arg567, Lys572, and Glu663). This implies that sucrose synthase shares not only a common origin with the GT-B family but also a similar catalytic mechanism. The enzyme preferred transferring glucose from ADP-glucose rather than UDP-glucose like the eukaryotic counterparts. This predicts that these prokaryotic organisms have a different sucrose metabolic scenario from plants. Nucleotide preference determines where the glucose moiety is targeted after sucrose is degraded.

IMPORTANCE

We obtained biochemical and structural evidence of sucrose metabolism in nonphotosynthetic bacteria. Until now, only sucrose synthases from photosynthetic organisms have been characterized. Here, we provide the crystal structure of the sucrose synthase from the chemolithoautotroph *N. europaea*. The structure supported that the enzyme functions with an open/close induced fit mechanism. The enzyme prefers as the substrate adenine-based nucleotides rather than uridine-based like the eukaryotic counterparts, implying a strong connection between sucrose and glycogen metabolism in these bacteria. Mutagenesis data showed that the catalytic mechanism must be conserved not only in sucrose synthases but also in all other retaining GT-B glycosyltransferases.

In plants, sucrose is a major photosynthetic product and plays a key role not only for carbon partition but also in sugar sensing, development, and regulation of gene expression (1–3). It was first thought that sucrose metabolism was a characteristic of plants, but it was later found in other oxygenic photosynthetic organisms (4, 5). In the last decade, Salerno and coworkers demonstrated the importance of sucrose for carbon and nitrogen fixation in filamentous cyanobacteria (6, 7). More recently, genomic and phylogenetic analyses revealed the existence of sucrose-related genes in nonphotosynthetic prokaryotes such as proteobacteria, firmicutes, and planctomycetes (4, 5, 8). It has been suggested that these organisms acquired the genes of sucrose metabolism by horizontal gene transfer (4, 5, 8). However, analysis of the enzymes encoded by such genes is currently lacking.

Nitrosomonas europaea is a chemolithoautotrophic bacterium that obtains energy by oxidizing ammonia to hydroxylamine and nitrite in the presence of oxygen (9). It is a member of the beta-proteobacteria group with a putative photosynthetic ancestor (10). *N. europaea* has potential for many biotechnological applications, including bioremediation of water contaminated with chlorinated aliphatic hydrocarbons (11) or ammonia, in combination with *Paracoccus denitrificans* (9). *N. europaea* displays some metabolic resemblance to photosynthetic organisms, but with marked differences. For instance, it possesses all the coding genes for enzymes of the Calvin-Benson cycle, but with two exceptions that could be replaced by other glycolytic enzymes (12). All the

genes coding for enzymes from the tricarboxylic acid cycle were found in *N. europaea* (12); however, activity of α -ketoglutarate dehydrogenase is nondetectable (13).

The evidence from genomic studies suggests that *N. europaea* can synthesize sucrose (12); however, the biochemical properties of enzymes from sucrose metabolism have not been characterized. Generally, in plants, sucrose is synthesized from UDP-glucose (UDP-Glc) and fructose-6-phosphate (Fru-6P) in a reaction catalyzed by sucrose-6-phosphate synthase (EC 2.4.1.14), followed by removal of the phosphate group by sucrose-6-phosphatase (EC

Received 17 February 2015 Accepted 19 May 2015

Accepted manuscript posted online 26 May 2015

Citation Wu R, Asención Díez MD, Figueroa CM, Machtey M, Iglesias AA, Ballicora MA, Liu D. 2015. The crystal structure of *Nitrosomonas europaea* sucrose synthase reveals critical conformational changes and insights into sucrose metabolism in prokaryotes. *J Bacteriol* 197:2734–2746. doi:10.1128/JB.00110-15.

Editor: A. M. Stock

Address correspondence to Dali Liu, dliu@luc.edu.

R.W., M.D.A.D., and C.M.F. contributed equally to this article.

Supplemental material for this article may be found at <http://dx.doi.org/10.1128/JB.00110-15>.

Copyright © 2015, American Society for Microbiology. All Rights Reserved.

doi:10.1128/JB.00110-15

3.1.3.24). The disaccharide can be degraded to Glc and Fru by invertases (EC 3.2.1.26) or cleaved by UDP to form UDP-Glc and Fru by sucrose synthase (NDP-glucose:D-fructose 2- α -D-glycosyltransferase [EC 2.4.1.13], also abbreviated as SUS or SuSy) (2, 3). However, some plant sucrose synthases have a certain degree of substrate promiscuity (14–21), while the one from *Thermosyn-echococcus elongatus* prefers ADP (16). For that reason, a general reversible reaction could be written as $\text{NDP} + \text{sucrose} \rightleftharpoons \text{NDP-Glc} + \text{Fru}$.

Besides its physiological role, sucrose synthase catalyzes a reversible reaction, and its activity can be measured in both directions *in vitro*. In filamentous cyanobacteria, the products derived from sucrose cleavage contribute to other biological processes, such as polysaccharide synthesis (22). Therefore, understanding the catalysis and the regulation of sucrose synthase is of great significance. Recently, Zheng et al. (23) reported the crystal structure of the *Arabidopsis thaliana* sucrose synthase in complex with UDP and fructose in a closed conformation. This enzyme is a homotetramer composed of four identical subunits of ~90 kDa and belongs to group 4 of the GT-B retaining glycosyltransferase family (<http://www.cazy.org/GlycosylTransferases.html>) (24). An S_Ni -like reaction mechanism has been proposed for this enzyme family (23–25).

Although several cyanobacterial (8, 16, 19) and plant (14, 17, 26–29) sucrose synthases have been characterized, the enzyme from nonphotosynthetic bacteria has never been studied, and no structural information on any sucrose synthase from bacterial sources is available. In this work we report the recombinant expression and biochemical characterization of *N. europaea* sucrose synthase and its crystal structure. We also determined the catalytic implications of highly conserved residues and the specificity for nucleotide substrates.

MATERIALS AND METHODS

Materials. Chemicals and coupled enzymes used for activity assays were from Sigma-Aldrich (St. Louis, MO). *Escherichia coli* BL21(DE3) cells were purchased from New England BioLabs (Ipswich, MA). Bacterial growth media and antibiotics were from Fisher Scientific (Pittsburgh, PA) and Sigma-Aldrich. Crystallization screen solutions and other supplies were purchased from Hampton Research (Aliso Viejo, CA) and Emerald Bio (Bedford, MA). All the other chemicals were of the highest quality available.

Cloning. The sequence (gene *ss2*, positions 1320268 to 1322652; GenBank accession number [AL954747](#)) coding for the sucrose synthase (NCBI accession number [CAD85125.1](#)) from *N. europaea* was amplified by PCR using genomic DNA from *N. europaea* ATCC 19718 as the template, the specific oligonucleotides CATATGACCACGATTGACACACTCGCCACCTGTACCC (forward, NdeI site underlined) and GTCGACTCATATCTCATGGGCCAGCCTGTTTGCCAGCGGCC (reverse, Sall site underlined) as primers, and Phusion HF DNA polymerase (Thermo Fisher Scientific, Rockford, IL) according to the manufacturer's instructions. The program used included an initial denaturation of 30 s at 98°C; 30 cycles of 98°C for 5 s, 50°C for 20 s, and 72°C for 2 min; and a final extension of 72°C for 5 min. The PCR product was purified after agarose gel electrophoresis and inserted into the pSC-B vector using the StrataClone Blunt PCR cloning kit (Agilent Technologies, Santa Clara, CA). Sequence identity was checked by automated DNA sequencing at CRC (Comprehensive Cancer Center at University of Chicago, IL). Afterwards, the sequence was subcloned into the pET28c vector (Merck KGaA, Darmstadt, Germany) between NdeI and Sall sites to obtain pNESS2, which is the plasmid that encodes the recombinant *N. europaea* sucrose synthase with an N-terminal His₆ tag.

Site-directed mutagenesis. Site-directed mutagenesis was performed by PCR overlap extension as previously described using Phusion DNA polymerase (30, 31). The plasmid encoding the *N. europaea* sucrose synthase (pNESS2) was used as a template for mutagenesis.

To introduce mutations in pNESS2 we used the following primers (mutated codons are in lowercase): TTACCATGGCGcgCTGGATCGGATC (forward) and GATCCGATCCAGcgCGCCATGGTAAA (reverse) for mutant R567A, CTGGATCGGATCcgAACATTACCGGC (forward) and GCCGGTAATGTTcgGATCCGATCCAG (reverse) for mutant K572A, and CCAGCCCTGTTcgGcGATTCCGGCCTG (forward) and CAGGCCGAATGcgGAAACAGGGCTGG (reverse) for mutant E663A. PCR conditions were the same as those described above. Flanking primers for the PCR overlap extension were the same as used for cloning (described above). All mutations were confirmed by DNA sequencing.

Protein expression and purification. Transformed *E. coli* BL21(DE3) cells with pNESS2 were grown in four flasks, each of them containing 1 liter of LB supplemented with 50 $\mu\text{g/ml}$ of kanamycin. This was performed in a 2.8-liter Fernbach flask at 37°C and 250 rpm until the optical density at 600 nm (OD_{600}) reached ~0.6. Protein expression was induced by the addition of 0.5 mM isopropyl- β -D-1-thiogalactopyranoside. Cells were incubated at 25°C and harvested after 16 h by centrifugation at 5,000 $\times g$ and 4°C for 15 min. The cell paste was resuspended in buffer C (20 mM Tris-HCl [pH 8.0], 200 mM NaCl, 5% [vol/vol] glycerol, 10 mM imidazole) and disrupted by sonication. The resulting suspension was centrifuged twice at 30,000 $\times g$ and 4°C for 15 min, and the soluble fraction (crude extract) was loaded onto a 5-ml HisTrap column (GE Life Sciences, Piscataway, NJ) containing Ni²⁺ and previously equilibrated with buffer C. Elution of the retained proteins was achieved with a linear imidazole gradient (20 column volumes, 10 to 300 mM). Fractions containing sucrose synthase activity were pooled, concentrated to 2 ml, and loaded onto a 16/60 Superdex 200 column (GE Life Sciences) previously equilibrated with 50 mM HEPES-NaOH (pH 8.0) and 300 mM NaCl. Fractions containing enzyme activity were pooled, concentrated, supplemented with 5% (vol/vol) glycerol, and stored at -80°C until use. Under these conditions, the enzyme remained stable and fully active for at least 3 months.

Protein assay and detection. Protein concentration was determined by measuring the protein absorbance at 280 nm using a NanoDrop 1000 (Thermo Fisher Scientific) and an extinction coefficient of 1.153 ml mg^{-1} cm^{-1} , determined from the amino acid sequence using the ProtParam server (<http://web.expasy.org/protparam/>). Denaturing protein electrophoresis was performed as described by Laemmli (32).

Enzyme assays. Activity assays were performed as previously described (16), with minor modifications. In the direction of sucrose synthesis, the reaction medium contained 50 mM 4-(2-hydroxyethyl)-1-piperazinepropanesulfonic acid (HEPPS; pH 8.0), 10 mM MgCl₂, 5 mM UDP-Glc, 500 mM Fru, 0.3 mM phosphoenolpyruvate, 0.3 mM NADH, 1 U of pyruvate kinase, 1 U of lactate dehydrogenase, 0.2 mg ml^{-1} of bovine serum albumin (BSA), and enzyme in an appropriate dilution in a final volume of 50 μl . Alternatively, activity was measured with 1 mM ADP-Glc and 20 mM Fru. NADH oxidation was followed by measuring the absorbance at 340 nm in a Multiskan Ascent microplate reader (Thermo Fisher Scientific) at 37°C. One unit of enzyme activity is defined as the amount of protein necessary to produce 1 μmol of product in 1 min under the specified conditions.

Kinetic characterization. Since the saturation kinetics of the enzyme were slightly sigmoidal, data of initial velocity (v) versus substrate concentration (S) were plotted and fitted to a modified Hill equation: $v = V_{\text{max}} S^{n_H} / (S_{0.5}^{n_H} + S^{n_H})$, where $S_{0.5}$ is the concentration of substrate necessary to obtain 50% of the maximal velocity (V_{max}) and n_H is the Hill coefficient. Fitting was performed by a nonlinear least-squares algorithm provided by the software Origin 7.0 (OriginLab Corporation). Kinetic parameters were obtained using the averages of two independent data sets that were reproducible within errors of $\pm 10\%$.

Phylogenetic analysis. We searched for protein sequences using the term “sucrose synthase” and applied the RefSeq filter in the National

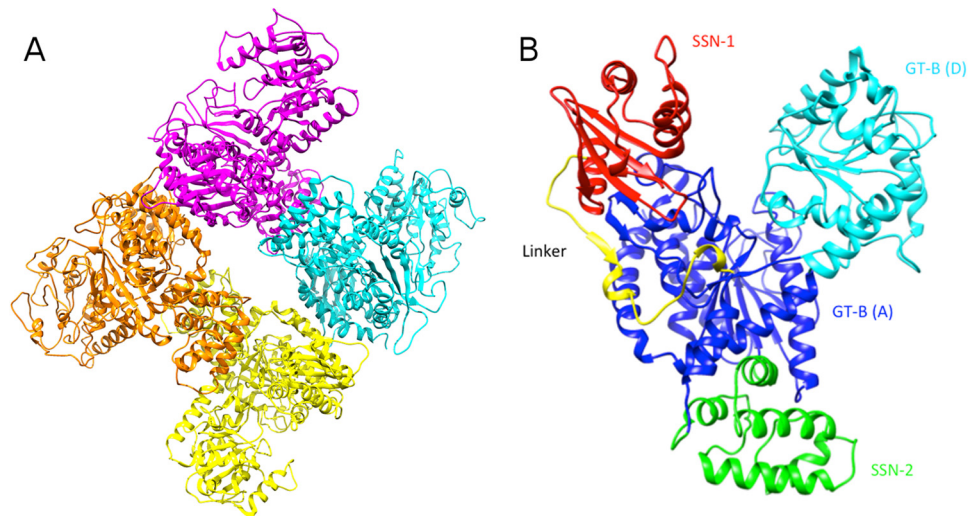


FIG 1 Crystal structure of the sucrose synthase from *N. europaea*. (A) Tetrameric structure of the enzyme. (B) Monomeric structure and its different domains: SSN-1, SSN-2, GT-B(A), and GT-B(D), and a linker between SSN-1 and SSN-2.

Center for Biotechnology Information (NCBI) database. Afterwards, we manually curated them to discard some which were clearly wrongly annotated since they had higher identity to other glycosyltransferases. Sequences were analyzed with the program BioEdit 7.0.5.3 (33) and aligned using the ClustalW server (<http://www.genome.jp/tools/clustalw/>). Tree reconstruction was performed using the neighbor-joining algorithm with a bootstrap of 1,000 in the program SeaView 4.4.0 (34). The tree figure was prepared using the FigTree 1.4.0 software (<http://tree.bio.ed.ac.uk/software/figtree/>).

Crystallization and data collection. After the initial crystallization screening and optimization, the recombinant protein was crystallized via the hanging-drop method. The hanging drops were prepared with 1 μ l of 15 mg ml⁻¹ sucrose synthase and 1 μ l of the reservoir solution, containing 5% Tacsimate (pH 5.0), 5% (wt/vol) polyethylene glycol 3350 (PEG 3350), and 0.1 M sodium citrate (pH 5.6). The hanging drops were kept at 20°C for crystallization. Crystals appeared in 3 days and were allowed to continue growing at 20°C for 4 more days, until they reached their maximum sizes. Crystals with good morphology and large sizes were transferred to a cryo-condition, which contained 25% glycerol in addition to the components of the reservoir solution, before being frozen in liquid nitrogen.

X-ray diffraction data sets were collected at the SBC19-ID beamline at the Advanced Photon Source (Argonne National Laboratory, Chicago, IL). The wavelength used in the monochromatic data collection was 1.008 Å. All the collected data sets were indexed and integrated using iMosflm and scaled with Scala in the CCP4 program suite (Collaborative Computational Project Number 4) (35). After investigating all statistic values indicating data quality, especially $I/\sigma\langle I \rangle$ and $CC_{1/2}$ (36), we decided to cut the data resolution at 3.05 Å, where $I/\sigma\langle I \rangle = 2$ while $CC_{1/2} = 0.561$, indicating good data quality (see Table 2).

Phasing, model building, and refinement. Molecular replacement was carried out using the program Phaser (37) from the CCP4 program suite. The starting search model in molecular replacement was modified from the known *A. thaliana* sucrose synthase structural model (PDB code 3S29) (23). The molecular replacement using the full-length *A. thaliana* sucrose synthase as a search model did not yield any solutions using Phaser. Suspecting that interdomain movement may have been the problem, we tried to virtually isolate some domains based on homology. Then, when we truncated the GT-B(D) domain (cyan domain in Fig. 1B) and used the rest of the molecule as the search model for molecular replacement in Phaser, a solution was finally obtained. Afterwards, model building was conducted in COOT (38). The GT-B(D) domain was built according to the electron density maps. Rigid body refinement and re-

strained refinement were conducted in re mac5 (39). In order to remove model bias and achieve the best refinement results possible, simulated annealing refinement and ordered solvent identification were conducted using PHENIX.refine (40).

Homology modeling. A model of the monomeric closed form of the *N. europaea* sucrose synthase (residues 16 to 788) was constructed with the program Modeller 9.11 (<https://salilab.org/modeller/>) (41). As a template we used the atomic coordinates of the *A. thaliana* sucrose synthase (3S27) with the ligands UDP and fructose (23). Before the modeling process, sequence alignment was performed manually to match functionally conserved residues and secondary structures. An identity of 50.3% ensured a high confidence alignment, since we only had to introduce four one-residue indels. The accuracy of the models was assessed with the Verify3D structure evaluation server (http://services.mbi.ucla.edu/Verify_3D/) (42).

Difference distance matrix map. We used an *ad hoc* program written in C applying previously developed concepts to detect domain motion and identify regions that move closer upon conformational changes (43). Distances were calculated between all pair of C_{α} of one reference structure (open), and a second pairwise distance matrix was calculated for the target (closed) structure. Afterwards, the target matrix was subtracted from the reference matrix to calculate the Δ distance plot (<https://github.com/ballicoragroup/didimama>).

Hinge analysis. In order to detect possible local conformations or hinges, we performed an analysis with the *ad hoc* program hingescan (<https://github.com/ballicoragroup/hingescan>). We compared the crystal structure of the open form of the *N. europaea* sucrose synthase with a closed-form homology model of the same enzyme. To detect if there is a significant local conformational change around a given residue (“hinge”), we extracted the coordinates of a given number (n) of C_{α} before the putative hinge and the same given number (n) of residues after (window size = $2n + 1$). This was done for both the open and closed forms and obtained two fragments to compare. After optimal rigid body superposition of only these two set of coordinates, an average distance was calculated (root mean square deviation [RMSD]). This RMSD calculated under these conditions was called the hinge score. When this score is at a peak, the “flanking” number of C_{α} at both sides displays a maximum change between the two structures. For that reason, a hinge is detected. The bigger the window, the bigger the domain movement is detected surrounding the hinge. To identify hinges that link small and bigger domains, different window sizes were scanned. A flowchart illustrating the process is in Fig. S1 in the supplemental material.

TABLE 1 Kinetic parameters of substrates of the *N. europaea* sucrose synthase in the synthesis direction^a

Substrate	$S_{0.5}$ (mM)	V_{\max} (U mg ⁻¹)	n_H	$k_{\text{cat}}/S_{0.5}$ (mM ⁻¹ s ⁻¹)
UDP-Glc	0.89 ± 0.05	4.3 ± 0.1	1.1	7.5
ADP-Glc	0.044 ± 0.006	3.7 ± 0.1	1.3	130.3
Fru _(UDP-Glc)	120 ± 10	2.8 ± 0.2	1.3	0.036
Fru _(ADP-Glc)	5.6 ± 0.4	4.8 ± 0.2	1.6	1.33

^a Assays were performed using the conditions described in Materials and Methods. Analogous values to catalytic efficiency ($k_{\text{cat}}/S_{0.5}$) were calculated using the predicted molecular mass of 93 kDa.

Glc. The $S_{0.5}$ for ADP-Glc is 0.044 mM in the presence of optimal concentrations of Fru (20 mM), whereas the $S_{0.5}$ for UDP-Glc is 0.98 mM in the presence of optimal concentrations of Fru (500 mM). On the other hand, the apparent affinity for Fru is higher in the presence of ADP-Glc rather than UDP-Glc. The $S_{0.5}$ for Fru at saturated concentrations of ADP-Glc is 5.6 mM, whereas the $S_{0.5}$ for Fru in the presence of UDP-Glc is significantly higher. Because of the high concentrations of Fru needed to reach saturation, it is not possible to measure the $S_{0.5}$ for Fru with high precision, but it is at least ~20-fold higher (120 mM). The catalytic efficiencies calculated for ADP-Glc and Fru_(ADP-Glc) were 17- and 37-fold higher than those obtained for UDP-Glc and Fru_(UDP-Glc), respectively (Table 1). These results indicate that the sucrose synthase from *N. europaea* prefers ADP-Glc over UDP-Glc as the substrate. Similar conclusions were obtained for the enzyme from the cyanobacterium *T. elongatus*, which showed a 26-fold higher catalytic efficiency for ADP-Glc than UDP-Glc (16). As it was stated for *T. elongatus* (16), this suggests that the metabolism of sucrose could be linked to the synthesis of glycogen, since ADP-Glc is the donor for its polymerization.

X-ray diffraction, data processing, model building, and refinement. The best data set collected at synchrotron beamline was processed to 3.05 Å and indexed as space group P65. It was integrated and scaled producing good statistics (Table 2). After the molecular replacement search, four copies of the starting model described in Materials and Methods were found in one asymmetric unit. Iterative cycles of model building and refinement were conducted, yielding a well-defined structure with R_{work} and R_{free} values of 17.37% and 21.75%, respectively (Table 2). The truncated GT-B(D) domain was built according to the electron density map. The final structural model contains all the residues except the first three at the N terminus and the last two at the C terminus of the amino acid sequence (Fig. 1).

Structural analysis of the sucrose synthase from *N. europaea*. (i) **Overall structure.** Although the resolution of the data set was 3.05 Å, the backbone of the protein and some of the key residues side chains were well defined by the electron density (see Fig. S3 and S4 in the supplemental material). This allowed us to conduct detailed structural analysis on sucrose synthase's conformational changes involving backbone movement, which are relevant to the catalytic cycle. The crystal structure displayed a fold similar to the previously reported structural model from the *A. thaliana* enzyme (PDB code 3S29) (23). The sucrose synthase from *N. europaea* is a tetramer composed of four identical subunits (Fig. 1A), where each monomer contains four domains (Fig. 1B).

The first domain, designated the sucrose synthase N-termi-

TABLE 2 Data collection and refinement statistics

Parameter	Value ^a
Data processing	
Space group	P65
Cell dimensions	
a, b, c (Å)	236.90, 236.90, 231.44
α, β, γ (°)	90.00, 90.00, 120.00
Resolution (Å)	3.05
Mosaicity (°)	0.47
R_{merge}^b	0.169 (0.963)
CC _{1/2}	0.993 (0.561)
I/σ	9.6 (2.1)
Completeness	97.9 (98.6)
Multiplicity	6.3 (6.3)
Refinement	
Resolution (Å)	3.05
No. of reflections	794,715
No. of unique reflections	126,170
$R_{\text{work}}/R_{\text{free}}^d$	17.37/21.75
RMSD ^e bond length (Å)	0.009
RMSD bond angle (°)	1.439

^a The values for the highest-resolution bin are in parentheses.

^b Linear $R_{\text{merge}} = \sum |I_{\text{obs}} - I_{\text{avg}}| / \sum I_{\text{avg}}$.

^c $R = \sum |F_{\text{obs}} - F_{\text{calc}}| / \sum F_{\text{obs}}$.

^d Five percent of the reflection data were selected at random as a test set, and only these data were used to calculate R_{free} .

^e RMSD, root mean square deviation.

nal 1 (SSN-1) domain, included residues 1 to 112 (Fig. 1B, red) and contained five α -helices and four β -strands. The second domain, which included residues 142 to 264, is the sucrose synthase N-terminal 2 (SSN-2) domain (Fig. 1B, green) with five α -helices. Domain SSN-1 and SSN-2 correspond to domains CTD and EPBD in the enzyme from *A. thaliana* (23). CTD and EPBD stand for “cellular targeting domain” and “ENOD40 peptide-binding domain,” which indicate the domain functions for the plant enzyme. In the case of the bacterial form, the roles for these domains are not known; thus, the nomenclature is based only on structure. Both the third and fourth domains constitute a typical GT-B fold of glycosyltransferases (24). The third is a domain that typically binds the nucleotide donor for the glycosyl group in that family (23, 25, 44). For this reason, we refer to it as GT-B(D) domain (Fig. 1B, cyan), although in sucrose synthase the transfer of glucosyl group is reversible. This nomenclature also matches the systematic name of the sucrose synthase (NDP-glucose:D-fructose 2- α -D-glucosyltransferase). The GT-B(D) domain includes residues 514 to 742, with eight α -helices and three β -strands. The fourth domain is the GT-B(A) domain (Fig. 1B, blue and yellow), which consists of residues from three separate regions. These separate regions are encompassed by the SSN-1, SSN-2, and GT-B(D) domains in the center of the monomer. The first region is a linker (residues 113 to 141) that joins SSN-1 and SSN-2 but structurally integrated to GT-B(A). The other two regions are residues 265 to 513 and residues 743 to 794. The GT-B(A) domain included nine α -helices and eight β -strands and functions in the GT-B family as the sugar acceptor (A) in catalysis (23, 25, 44).

As mentioned above, the identity between sequences from *N. europaea* and *A. thaliana* is considerably high (50.3%). When the different domains were analyzed separately, we found identity values of 26.2% for SSN-1 (CTD), 40.2% for SSN-2 (EPBD), 52.4%

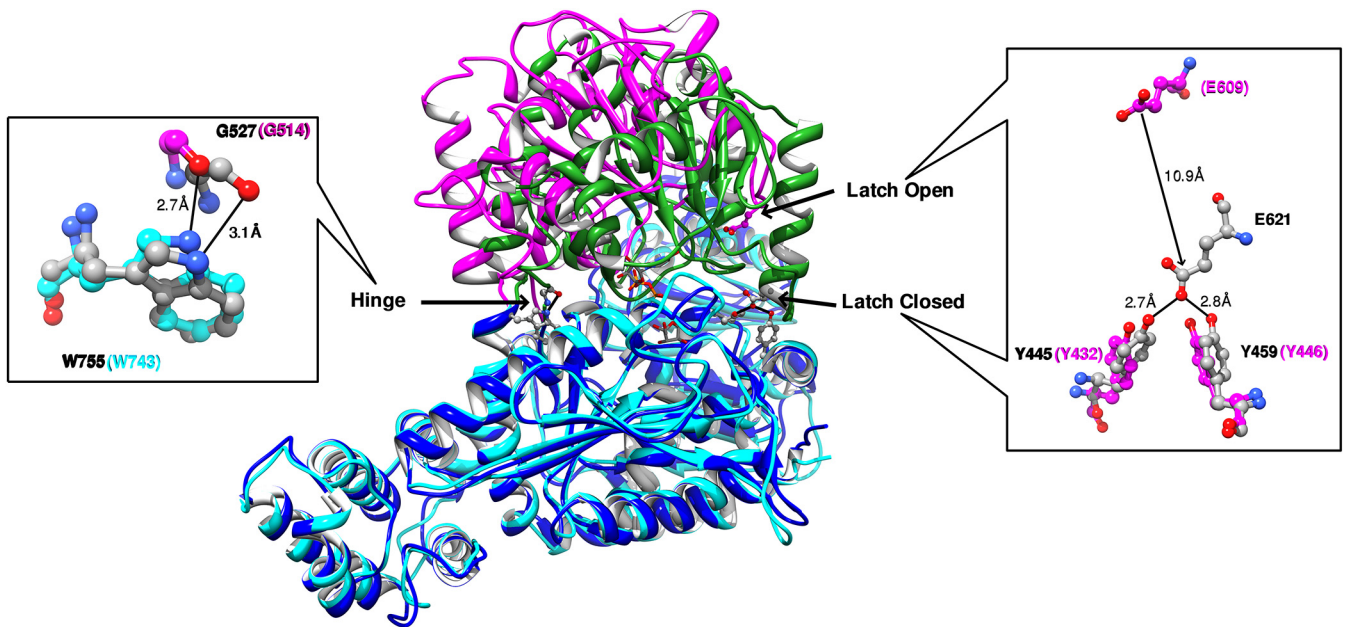


FIG 3 Comparison of the open and closed monomeric forms. The open-form structure is represented by the *N. europaea* sucrose synthase structure reported in this paper; the closed form is represented by the *A. thaliana* enzyme (PDB code 3S29). The SSN-1, SSN-2, and GT-B(A) domains are shown in blue for the open-form structure and in cyan for the closed-form structure. The GT-B(D) domain is shown in magenta for the open form and in green for the closed form. The hinge-latch features of the domain movement are shown in enlarged views.

for GT-B(D), and 61.9% for GT-B(A), suggesting a high structural conservation. A comparison between the *A. thaliana* and *N. europaea* X-ray structures confirms it. With the exception of conformational changes, each of the folds for their respective domains is identical. The fact that the structure is so conserved, even for the domains that are not related to catalysis, would suggest that certain noncatalytic functional roles have been preserved or adapted. On the other hand, SSN-1 (CTD in *A. thaliana*) does not have the Ser that is phosphorylated in plants, indicating that it is a role acquired in eukaryotes. Therefore, it is not certain whether *N. europaea* sucrose synthase is regulated for binding macromolecular structures such as actin or membranes as plant enzymes do (26, 45). Prokaryotes do not have cytoskeleton, although actin-related proteins have been detected in *Anabaena* species (46). Whether sucrose synthase from bacteria can actually interact with actin or similar structures is a matter for further studies.

In *N. europaea*, SSN-2 is involved in the oligomerization forming one of the contacts between subunits. It is not clear if it has any other physiological role. In *A. thaliana*, EPBD (SSN-2 in *N. europaea*), together with the CTD domain (SSN-1 in *N. europaea*), forms a groove hypothesized to bind actin (23). In our structure, the same structural arrangement is present (data not shown), highlighting the possibility that a similar role has been conserved. However, this needs to be investigated.

The obtained *N. europaea* sucrose synthase structure with no substrates bound has an overall conformation clearly different from that of the *A. thaliana* structure with UDP and Fru (23). This implies that substrate binding induces significant conformational changes (Fig. 3), and it correlates with similar conformational changes that occur upon binding of substrates in other GT-B retaining glycosyltransferases (25, 47). After superimposition of only the GT-B(A) domains of the *A. thaliana* and *N. europaea* structures (using the least-squares function in COOT), the SSN-1,

SSN-2, and GT-B(A) domains overlapped well, while the GT-B(D) domains were in a different relative position. The angle between the GT-B(A) and GT-B(D) domains in the obtained structure was about 23.5 degrees wider than in *A. thaliana*. Based on such comparison, we suggest that the *N. europaea* structure in this work was in an “open” conformation, whereas the *A. thaliana* form was “closed” (23). We have identified some distinct structural determinants (hinges and latches) related to the movements of the sugar [GT-B(A)] and nucleotide [GT-B(D)] binding domains.

(ii) Sugar-binding GT-B(A) domain. We compared the open structure crystal structure of *N. europaea* enzyme with the homology model in a closed conformation built as described in Materials and Methods. Considering how modeling works, and that the closed structure template (*A. thaliana*) has no gaps with the *N. europaea* target in the sites of interest, the backbone comparison with the model is as reliable as comparing the backbones of both structures directly. The RMSD of backbone between the model obtained and the closed *A. thaliana* template was 0.29 Å. However, the use of the model is more convenient since the number is not shifted, which would be really confusing in the following analysis. One of the important assumptions we make is that the closed structure of the *A. thaliana* enzyme is a fair representation of the closed structure of that from *N. europaea*. We believe that this is a reasonable assumption, at least in the critical areas. Otherwise, the backbone of critical residues may not align properly for catalysis.

Analysis of a difference distant matrix map of the Fru-binding GT-B(A) domain as described in Materials and Methods highlights three main regions that move closer upon sugar binding (Fig. 4). These are residues 325 to 375 to residues 280 to 290 (~5 Å), residues 425 to 435 to residues 280 to 290 (~4 Å), and residues 425 to 435 to residues 325 to 375 (~3 Å) (Fig. 4). Other pair of regions that move toward each other are residues 280 to 290 to

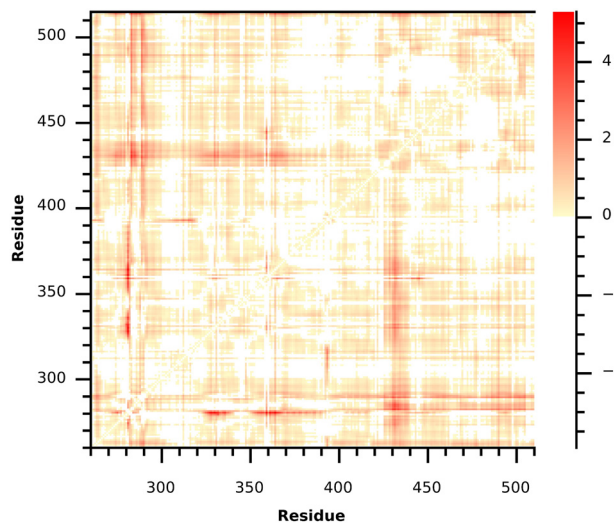


FIG 4 Difference distance matrix map of the GT-B(A) domain. Distances were calculated between all pair of C_{α} carbon of the open structure (*N. europaea* sucrose synthase). A second pairwise distance matrix was calculated for the closed structure (homology model as described in Materials and Methods). Afterwards, these two matrices were subtracted, and the Δ distance was color coded. The negative and zero values are represented in white. Red colors (higher Δ distance values) are pairs of C_{α} carbon that are getting closer upon closing of the enzyme. Only residues from 260 to 510 are shown, which correspond to the GT-B(A) domain.

residues 490 to 505 (~ 3 Å) and residues 280 to 290 to residues 450 to 460 (~ 2 Å) (Fig. 4). From this analysis, the area from residues 280 to 290 is the most involved in an induced fit interaction with Fru. Further inspection of these areas reveals that Fru induces local conformational changes via superimposition of the GT-B(A) domains of the *A. thaliana* (closed) and the *N. europaea* (open) sucrose synthases (Fig. 5). These include the side chain of K431

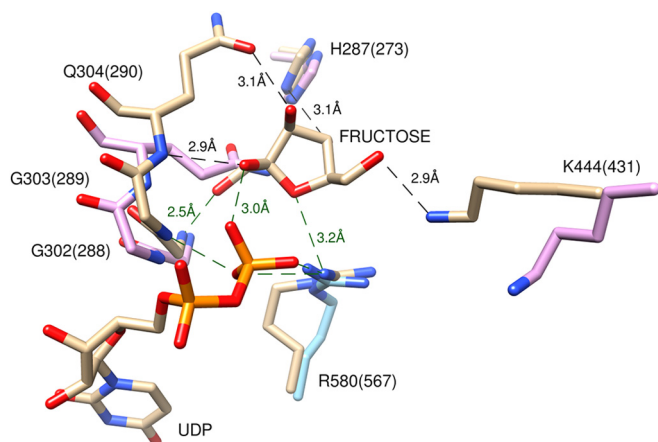


FIG 5 Overlap comparison of the fructose binding sites of the open (*N. europaea*) and closed (*A. thaliana*; PDB code 3S29) sucrose synthase structures. The carbon atoms in the closed form structure are in pale yellow. The carbon atoms in the open form structure are in cyan [GT-B(A) domain] and pink [GT-B(D) domain]. Conserved residues between two structures are labeled with respective residue numbers; the residue numbers of the open-form structure are in parentheses. The hydrogen bonds in the GT-B(D) domain are shown in black. The hydrogen bonds in between GT-B(A) and GT-B(D) domains and the ones in GT-B(A) domains are shown in green.

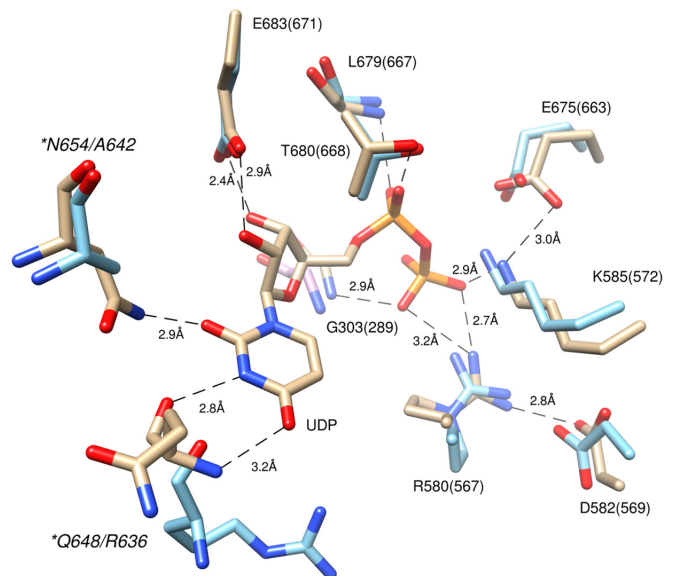


FIG 6 Overlap comparison of the nucleotide binding sites of the open (*N. europaea*) and closed (*A. thaliana*; PDB code 3S29) sucrose synthase structures. The carbon atoms in the closed-form structure are in pale yellow. The carbon atoms in the open-form structure are in cyan [GT-B(A) domain] and pink [GT-B(D) domain]. Conserved residues between two structures are labeled with respective residue numbers; the residue numbers of the open-form structure are in parentheses. The asterisks indicate the nonconserved binding residues, with the closed-form residues labeled in front of the ones in the open-form structure.

and the backbone of residues 288 to 290. The reshaping of the Fru binding site facilitates the closing via a set of interdomain hydrogen bonds (Fig. 5, in green). These local conformational changes along with the presence of Fru further promote the interactions between the GT-B(A) and GT-B(D) domains. Thus, we propose that Fru binding contributes to stabilizing the closed structure.

(iii) **Nucleotide binding GT-B(D) domain.** The GT-B(D) domain binds to sugar nucleotide (synthesis direction) or nucleotide (cleavage direction) substrates. When the GT-B(D) domains from both *A. thaliana* and *N. europaea* structures overlap, the residues interacting with the phosphate and ribose moieties of the nucleotides are not only conserved but also at the same positions (Fig. 6). On the other hand, two residues interacting with the nucleotide base are not conserved. Residues Q648 and N654 from the *A. thaliana* are replaced by R636 and A642 in the *N. europaea* sucrose synthase, respectively. This difference creates a more spacious binding site in *N. europaea*, which may accommodate bulkier adenosine nucleotide substrates. Modeling an ADP ligand into the *N. europaea* structure shows that the site may have a deeper pocket, which would be needed not to clash with the adenine ring (Fig. 6 and 7). Similar sequence differences were observed in the sucrose synthase from *T. elongatus* (16). Based on sequence analysis and homology modeling, it was suggested that these two residues could be responsible for the preference toward ADP/ADP-Glc over other nucleotides such as UDP/UDP-Glc in the cyanobacterial enzyme (16). It is important to note that the side chains in R636 and A642 in the *N. europaea* sucrose synthase are not conserved in the *E. coli* glycogen synthase, which is another glycosyltransferase that binds ADP-Glc (48). *E. coli* glycogen synthase has a different motif in that position, with a Tyr and Ser instead of Arg

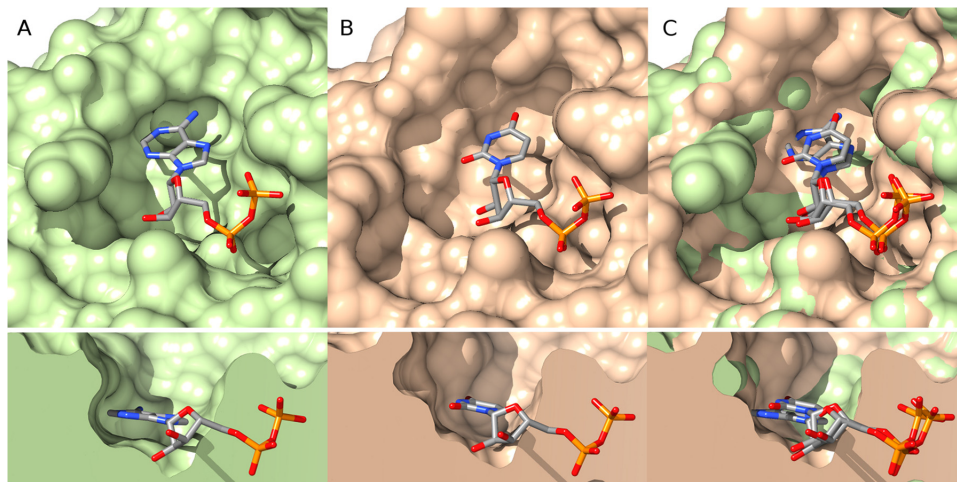


FIG 7 Modeling of the ADP-Glc binding site. Panel A shows the GT-B(D) domain of the *N. europaea* sucrose synthase, in which ADP has been modeled with Modeller. For that purpose, the closed structure of glycogen synthase with ADP bound (PDB code 2QZS) was manually aligned to the closed structures of *A. thaliana* (PDB codes 3S27 and 3S28) and the structure from *N. europaea* (this work). All those alignments were used as the templates. Loops that did not structurally align well were not used for the modeling, and the backbone structure was inherited from the *A. thaliana* structures. The rest of the modeling and validation proceeded as described in Materials and Methods. Panel B shows the GT-B(D) domain from *A. thaliana* (PDB code 3S27) and the UDP bound.

and Ala (25, 47, 48), implying a different structural arrangement for accommodating ADP-Glc. Overall, the nucleotide binding to the GT-B(D) domain does not seem to trigger significant local conformational changes (Fig. 6). The direct interactions with the nucleotide do not make major contributions to the induced fit mechanism.

(iv) Hinge analysis. We scanned the structures of the acceptor and donor domains for hinges and subtle conformational changes that could be functionally important in catalysis. We used the in-house program hingescan described in Materials and Methods. Using several window sizes, we detected several local conformational changes (see Fig. S5 in the supplemental material). For a

window size of 51, we detected two clear hinge elements near residues ~ 515 and ~ 744 (Fig. 8). These two elements actually form a single “hinge” that comprises a hydrogen bond between two conserved residues (G514 and W743) in a flexible area (Fig. 3; see also Fig. S4 and S5). These two residues remain at the same position in both the open and the closed conformations of the enzyme. For smaller windows, we found other significant local secondary-structure rearrangements between the open and closed structures (Fig. 8; see also Fig. S5 and S6). Upon closing, two α -helices in the GT-B(D) domain are extended, and a β -strand replaces a previously coiled stretch. The outcome is a more ordered structure of the GT-B(D) domain. We propose that this

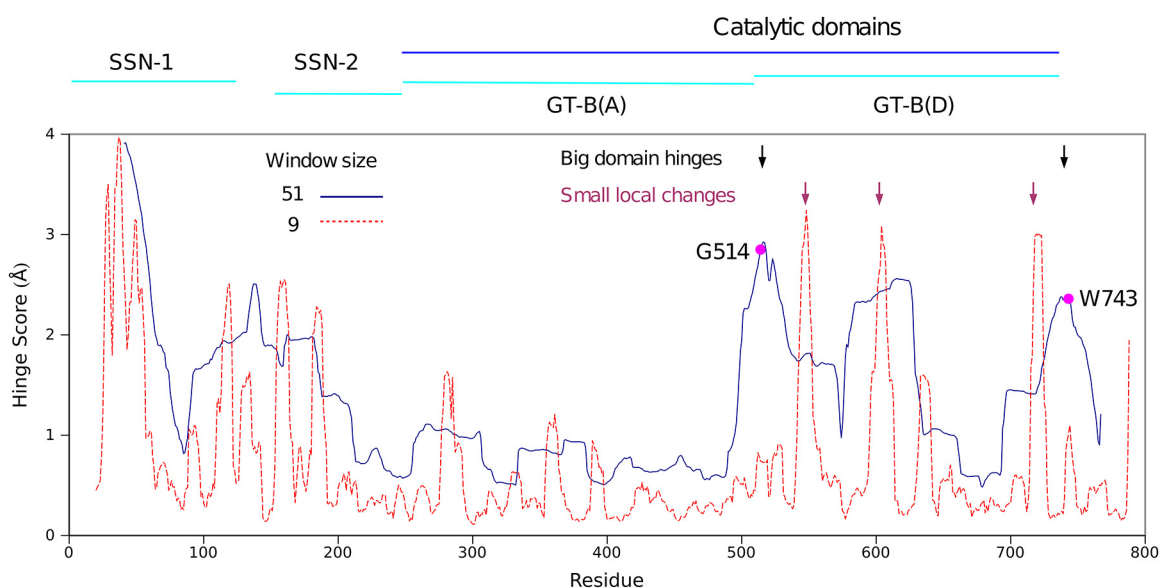


FIG 8 Hinge analysis by comparison of the open versus closed conformations. The blue and red show the hinge score using 51 and 9 windows, respectively. The magenta dots (also black arrows) show the two distinct hinges: G514 and W743. The purple arrows point at the region displaying the secondary-structure rearrangements.

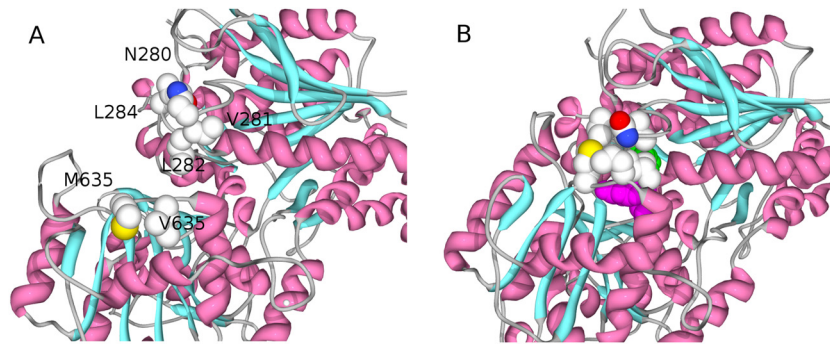


FIG 9 Hydrophobic residues contribute to the latch action. Panel A depicts the open structure (*N. europaea* sucrose synthase crystal structure), and panel B depicts a homology model of a closed structure, which was built as described in Materials and Methods. Upon closing, the hydrophobic residues M635 and L637 in the GT-B(D) domain and N280, V281, L282, and L284 in the GT-B(A) domain generate a hydrophobic environment that stabilizes the close action.

secondary-structure rearrangement, despite the local entropy decrease, would release extra energy to close the conformation, facilitating the binding of substrates.

There are also differences between the conformations of the SSN-1 and SSN-2 domains from the open structure of the *N. europaea* enzyme and the model of the closed form (Fig. 8). The analysis detected hinges because of local differences, and there are four major regions with scores above 2 (Fig. 8; see also Fig. S5 and S7 in the supplemental material). This predicts that some of the loops in these two domains are quite flexible, but we cannot assign a functional role to them (see Fig. S7). In *A. thaliana*, the flexibility of the CTD domain (SSN-1) is hypothesized to have a role in actin binding (23).

(v) **Latches.** A feature that contributes to the stabilization of the closed form is a “latch,” E609, which comprises the highly conserved E609 residue located at the periphery of the GT-B(D) domain (see Fig. S2 in the supplemental material). Going from an open to a closed conformation, this glutamate residue moves ~ 11 Å toward the GT-B(A) domain and ends up hydrogen bonded to two tyrosine residues (Y432 and Y446) stabilizing the closing (Fig. 3; see also Fig. S8). Interestingly, there were small secondary-structure rearrangements in the vicinity of this latch, which could facilitate the interaction between E609 and the two tyrosines (see Fig. S6). On the other side of the active site, opposite to the latch described, there is a hydrophobic patch that also contributes to the closing (Fig. 9). Two hydrophobic residues (M635 and L637) in the GT-B(D) domain get in contact with a hydrophobic cluster (V281, L282, and L284) in the GT-B(A) domain upon closing. The side chain of N280 also provides a methylene to build a nonpolar pocket that latches on to M635 and L637 (Fig. 9). On the other hand, the amide polar group is exposed to the solvent.

The closed structure seems to induce stronger interactions with the nucleotide and vice versa. In the *N. europaea* sucrose synthase, the conserved E671 is in the same position as E369 in the *E. coli* trehalose-6-phosphate synthase (OtsA) (48, 49). In OtsA, as well as in the close conformation of the *A. thaliana* sucrose synthase (E683), the carboxylate of this side chain forms two hydrogen bonds with the hydroxyl groups of the ribose of the nucleotide. In these enzymes, the carboxylate is surrounded by hydrophobic residues (Y520, Y646, L667, and T668 in *N. europaea* sucrose synthase; Y533, Y658, L679, and T680 in the *A. thaliana* enzyme), which makes the hydrogen bonds stronger in the nonpolar environment. In the open form of the sucrose synthase

structure, V291 (V306 in *A. thaliana*) moves away from the side chain of the glutamate residue (see Fig. S9 in the supplemental material). This implies that the closing recruits a nonpolar side chain to completely surround the carboxylate. Consequently, nucleotide binding stabilizes the carboxylate charge and facilitates the interaction with V291 upon closing. Interestingly, in another glycosyltransferase, bacterial glycogen synthase, E671 was replaced by a Tyr, and V291 was replaced by Asp, thus switching their roles (48). Therefore, this ligand-dependent interaction may be a common feature in this family of enzymes.

Site-directed mutagenesis of critical residues. Previously, important residues for catalysis were identified in other retaining GT-B glycosyltransferases. A triad of critical residues has been found in the active site of maltodextrin phosphorylase (50, 51) and glycogen synthase from *E. coli* (52). Based on X-ray structures, these residues were also predicted to be important for catalysis in OtsA (49) and the *A. thaliana* sucrose synthase (23). The homologous residues in *N. europaea* are R567, K572, and E663 (Fig. 10). When any of those residues was replaced by alanine, the activity in the direction of sucrose synthesis severely decreased in the presence of either ADP-Glc or UDP-Glc (Table 3). The most active of all these mutants was the E663A mutant in the presence of ADP-Glc, but it was still 200-fold less active than the wild type. These results indicate that this triad is critical in sucrose synthases. Consequently, they also suggest that sucrose synthases together with all other retaining glycosyltransferases with a GT-B fold share the same reaction mechanism (Fig. 10).

Structural and mechanistic consequences of the open/closed conformational change. Large conformational movements may have a large impact on the architecture of the active site. For that reason, it is important to analyze how critical catalytic residues are arranged in the closed and open structures of sucrose synthase. We have identified and confirmed by mutagenesis three critical side chains in *N. europaea* sucrose synthase (R567, K572, and E663, corresponding to R580, K485, and E675 in *A. thaliana*). In addition, the comparison with other glycosyltransferases predicts another interaction (protein backbone-substrate) that stabilizes the transition state (24), which is not possible replaced through mutagenesis. The comparison between the open and closed forms of *N. europaea* and *A. thaliana* sucrose synthases, respectively, provides important information. But the arrangement of the critical residues needs to be put in context of the reaction mechanism.

It has been proposed that retaining glycosyltransferases have

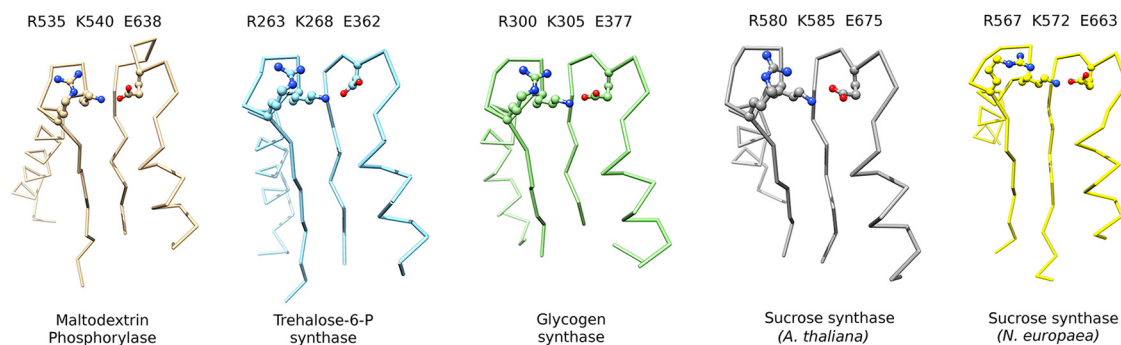


FIG 10 Three highly conserved catalytic residues in different members of the retaining GT-B glycosyltransferase family. The structures analyzed are maltodextrin phosphorylase (PDB code 1E4O), trehalose-6-phosphate synthase (PDB code 1GZ5), and glycogen synthase (PDB code 2QZ5) from *E. coli*, sucrose synthase from *A. thaliana* (PDB code 3S29), and *N. europaea* (this work).

either an S_Ni -like mechanism with an oxocarbenium-phosphate short-lived ion pair intermediate or an S_Ni mechanism forming an oxocarbenium ion-like transition state that is not totally dissociated from the donor and acceptor (24, 53, 54). In either of those two cases, an important stabilization of the transition state would be based on the interaction between the anomeric carbon (C-1) of the sugar being transferred and the oxygen of the main chain of a His residue (24, 55). Recently, an alternative elimination/addition mechanism has been proposed for the *Pyrococcus abyssi* glycogen synthase (56), which was argued to be compatible with the currently available data. In this mechanism, a general base is needed to extract a proton from C-2 of the glycosyl group. The authors proposed this base is the same main-chain oxygen from the His residue as mentioned above. Interestingly, in the crystal structure of the *A. thaliana* sucrose synthase, the oxygen of the main chain of H438 (H425 in *N. europaea*) is at a close distance of both C-1 and C-2 of a proposed 1,5-anhydro-D-arabino-hex-1-enitol (see Fig. S10 in the supplemental material). This ligand mimics the planar structure of the transition state in either the S_Ni , S_Ni -like, or elimination/addition mechanism (56). This type of *in situ*-generated intermediate was also observed in the *E. coli* and *P. abyssi* glycogen synthases (25, 56). Regardless of these alternative mechanisms, it must be critical that the main-chain oxygen of H425 in *N. europaea* sucrose synthase is near C-1/C-2 in the transition state. Since this residue is located in the GT-B(A) domain, and there are other critical residues in GT-B(D) (Table 3), a precise arrangement between these two domains is necessary for a proper architecture of the catalytic site. Only in the closed structure would all these functional groups be at the right distance for catalysis (see Fig. S10). Therefore, one of the roles of the closing is to bring the critical residues to a proper position.

It is tempting to argue that UDP-Glc/ADP-Glc can induce the closing, based on the fact that the base and the ribose have numer-

ous contacts with the GT-B(D) domain and the glycosyl group with the opposing GT-B(A) domain (23). However, it is not clear how stable the closed form would be in the presence of the donor without the acceptor. During the crystallization process, the *A. thaliana* enzyme cleaves UDP-Glc to generate UDP and possibly 1,5-anhydro-D-arabino-hex-1-enitol (or its tautomer 1,5-anhydro-D-fructose), yielding a closed structure (23). But this structure, which could occur transiently, may have been driven and stabilized by the extremely slow generation of 1,5-anhydro-D-arabino-hex-1-enitol. It is expected that this putative transition state analog binds favorably to the most active form of the enzyme, which in this case is the closed one.

The rationale for a conformational change induced by substrates (“induced fit”) was first described by Koshland to explain why a specific (good) substrate reacts faster than smaller (poor) alternatives that can also fit into the active site (57). If the changes that lead to a precise orientation of catalytic groups only occur upon binding of the (good) substrate, another (poor) substrate that does not trigger those conformational changes will not react effectively, even at high concentrations. This concept, or at least its interpretation, has been controversial (58, 59). On the other hand, Fersht stated that an induced fit mechanism does not increase substrate specificity *per se* (59), and the only contribution that matters is the relative binding affinities to the transition states of the competing reactions. According to this, to increase the sucrose synthase specificity for the acceptor Fru against water, selective interactions seems to be maximized by surrounding Fru completely by different functional groups from the enzyme. Consequently, the active site is isolated from the solution as shown in Fig. S11 in the supplemental material. For that reason, an induced fit mechanism becomes an indirect necessity to allow substrates and products to enter and leave, while maximizing a selective interaction with Fru.

For retaining glycosyltransferases, another key issue is the stabilization of the β -phosphate to make it a better leaving group (54, 60). A hydroxyl group from the acceptor (Fru in this case) participates in a hydrogen bond with the β -phosphate. Consequently, the oxygen of this group becomes a better nucleophile to attack the C-1 of the forming oxocarbenium ion (54). Water could, in theory, compete with the acceptor (Fru) for this role, but is a poor substrate, probably because it does not stabilize the closed structure as well as Fru does. Fru not only interacts with the phosphate leaving group but also interacts more tightly with the closed form.

TABLE 3 Activities of wild-type and mutant forms of the *N. europaea* sucrose synthase^a

Substrate	V_{max} (U mg ⁻¹)			
	WT	R567A	K572A	E663A
UDP-Glc	4.3 ± 0.1	<0.0017	<0.0019	<0.01
ADP-Glc	3.7 ± 0.1	<0.0014	<0.0016	0.020 ± 0.02

^a Assays were performed using the conditions described in Materials and Methods. WT, wild type.

Not only do the distances between the residues in the GT-B(A) domain that contact Fru get closer upon closing but also networks of interactions of Fru with the GT-B(D) domain are established (Fig. 6; see also Fig. S11 in the supplemental material). Noteworthy are the interaction of Fru with R580 (*A. thaliana*) and the hydrogen bond with K444 that brings Y445 closer to E621, forming the latch (see Fig. S11D and E). Interestingly, the closed structure of the *A. thaliana* enzyme with the cleaved products of UDP-Glc seems to shape the active site to readily accommodate Fru. Even if Fru is absent, the site is nearly identical to the structure with Fru bound (see Fig. S11, RMSD 0.27 °). On the other hand, the structure of the open form of the *N. europaea* enzyme does not have all these residues at a proper distance to bind Fru (see Fig. S11C). This indicates that Fru would preferentially bind to the closed form, stabilizing it.

This mechanism in which the catalytic residues get into places upon closing may explain why it is not trivial to obtain a closed structure with an intact sugar nucleotide. For instance, crystal structures of the closed forms were obtained for the *E. coli* glycogen synthase and the *A. thaliana* sucrose synthase grown in presence the sugar nucleotide, but the glycosyl group was slowly cleaved (23, 25, 56). There are other retaining GT-B structures with a sugar nucleotide bound, but those were described as “semi-closed” (44). A mechanism with a domain movement that allows the exchange of ligands to the solution is not unique for sucrose synthase and may be general among retaining GT-B enzymes. However, not all of them may require such a large conformational change. The glycogen synthase was another case with closed and wide open structures described (25, 47, 56). The sucrose-6-phosphate synthase must also have the same type of behavior, but only an open structure is available (61). In other cases, open/closed structures have been obtained, but the most significant movements were local rearrangement of loops (rather than a large domain rearrangement) such as in OtsA (44) and VldE (62, 63).

Conclusions. In this study, we observed an open conformation for sucrose synthases. Based on the comparison with a previously published closed sucrose synthase structure (23), a hinge-latch combination was identified as a critical feature responsible for the open-close enzyme actions.

We identified three highly conserved amino acids proposed to be critical for catalysis. We concluded that the triad composed of residues R567, K572, and E663 (numbers according to the *N. europaea* enzyme) plays a key role not only in sucrose synthases but also in all the retaining GT-B glycosyltransferases (23, 49–52).

With both structural and kinetic results, we propose that the sucrose synthase from *N. europaea* has a substrate preference in favor of ADP/ADP-Glc over UDP/UDP-Glc. This behavior is similar to that observed for *T. elongatus* sucrose synthase (16).

The evolutionary origin of enzymes from sucrose metabolism in proteobacteria has been previously discussed (4, 5, 8, 64). The evolution of sucrose synthases in cyanobacteria, proteobacteria, and plants is not yet fully understood, but most likely it involved horizontal gene transfers. On one hand, the sucrose synthase from *N. europaea* is closer to the plant enzymes in the phylogenetic tree (Fig. 2), but on the other hand, the specificity for nucleotides is similar to that for several cyanobacterial enzymes evolved (8, 16). It is possible that the enzyme from *N. europaea* examed from a protein already present in the common ancestor of proteobacteria and cyanobacteria (10).

ACKNOWLEDGMENTS

This work was supported by grants from ANPCyT (PICT'12 2439) and CONICET (PIP 112-201101-00438) to A.A.I., UNL (CAI+D 2011) to C.M.F. and A.A.I., NSF (MCB-1024945) to M.A.B., and NSF (CHE-1308672) to D.L. M.D.A.D., C.M.F., and A.A.I. are researchers from CONICET.

REFERENCES

- Koch K. 2004. Sucrose metabolism: regulatory mechanisms and pivotal roles in sugar sensing and plant development. *Curr Opin Plant Biol* 7:235–246. <http://dx.doi.org/10.1016/j.pbi.2004.03.014>.
- Lunn JE. 15 December 2008. Sucrose metabolism. eLS <http://dx.doi.org/10.1002/9780470015902.a0021259>.
- Winter H, Huber SC. 2000. Regulation of sucrose metabolism in higher plants: localization and regulation of activity of key enzymes. *Crit Rev Biochem Mol Biol* 35:253–289. <http://dx.doi.org/10.1080/10409230008984165>.
- MacRae E, Lunn J. 2012. Photosynthetic sucrose biosynthesis: an evolutionary perspective, p 675–702. In Eaton-Rye JJ, Tripathy BC, Sharkey TD (ed), *Photosynthesis*, vol 34. Springer, Dordrecht, Netherlands.
- Salerno GL, Curatti L. 2003. Origin of sucrose metabolism in higher plants: when, how and why? *Trends Plant Sci* 8:63–69. [http://dx.doi.org/10.1016/S1360-1385\(02\)00029-8](http://dx.doi.org/10.1016/S1360-1385(02)00029-8).
- Cumino AC, Marcozzi C, Barreiro R, Salerno GL. 2007. Carbon cycling in *Anabaena* sp. PCC 7120. Sucrose synthesis in the heterocysts and possible role in nitrogen fixation. *Plant Physiol* 143:1385–1397.
- Curatti L, Giarocco L, Salerno GL. 2006. Sucrose synthase and RuBisCo expression is similarly regulated by the nitrogen source in the nitrogen-fixing cyanobacterium *Anabaena* sp. *Planta* 223:891–900. <http://dx.doi.org/10.1007/s00425-005-0142-7>.
- Kolman MA, Torres LL, Martin ML, Salerno GL. 2012. Sucrose synthase in unicellular cyanobacteria and its relationship with salt and hypoxic stress. *Planta* 235:955–964. <http://dx.doi.org/10.1007/s00425-011-1542-5>.
- Yamanaka T. 2008. Chemolithoautotrophic bacteria: biochemistry and environmental biology. Springer, Tokyo, Japan.
- Teske A, Alm E, Regan JM, Toze S, Rittmann BE, Stahl DA. 1994. Evolutionary relationships among ammonia- and nitrite-oxidizing bacteria. *J Bacteriol* 176:6623–6630.
- Vannelli T, Logan M, Arciero DM, Hooper AB. 1990. Degradation of halogenated aliphatic compounds by the ammonia-oxidizing bacterium *Nitrosomonas europaea*. *Appl Environ Microbiol* 56:1169–1171.
- Chain P, Kurtz S, Ohlebusch E, Slezak T. 2003. An applications-focused review of comparative genomics tools: capabilities, limitations and future challenges. *Brief Bioinform* 4:105–123. <http://dx.doi.org/10.1093/bib/4.2.105>.
- Hooper AB. 1969. Biochemical basis of obligate autotrophy in *Nitrosomonas europaea*. *J Bacteriol* 97:776–779.
- Baroja-Fernández E, Muñoz FJ, Saikusa T, Rodríguez-López M, Akazawa T, Pozueta-Romero J. 2003. Sucrose synthase catalyzes the de novo production of ADP-glucose linked to starch biosynthesis in heterotrophic tissues of plants. *Plant Cell Physiol* 44:500–509. <http://dx.doi.org/10.1093/pcp/pcp062>.
- Delmer DP. 1972. The purification and properties of sucrose synthetase from etiolated *Phaseolus aureus* seedlings. *J Biol Chem* 247:3822–3828.
- Figueroa CM, Asencion Diez MD, Kuhn ML, McEwen S, Salerno GL, Iglesias AA, Ballicora MA. 2013. The unique nucleotide specificity of the sucrose synthase from *Thermosynechococcus elongatus*. *FEBS Lett* 587:165–169. <http://dx.doi.org/10.1016/j.febslet.2012.11.011>.
- Grimes WJ, Jones BL, Albersheim P. 1970. Sucrose synthetase from *Phaseolus aureus* seedlings. *J Biol Chem* 245:188–197.
- Morell M, Copeland L. 1985. Sucrose synthase of soybean nodules. *Plant Physiol* 78:149–154. <http://dx.doi.org/10.1104/pp.78.1.149>.
- Porchia AC, Curatti L, Salerno GL. 1999. Sucrose metabolism in cyanobacteria: sucrose synthase from *Anabaena* sp. strain PCC 7119 is remarkably different from the plant enzymes with respect to substrate affinity and amino-terminal sequence. *Planta* 210:34–40. <http://dx.doi.org/10.1007/s004250050651>.
- Ross HA, Davies HV. 1992. Purification and characterization of sucrose synthase from the cotyledons of *Vicia faba* L. *Plant Physiol* 100:1008–1013.
- Tanase K, Yamaki S. 2000. Purification and characterization of two sucrose synthase isoforms from Japanese pear fruit. *Plant Cell Physiol* 41:408–414. <http://dx.doi.org/10.1093/pcp/41.4.408>.

22. Curatti L, Giarrocco LE, Cumino AC, Salerno GL. 2008. Sucrose synthase is involved in the conversion of sucrose to polysaccharides in filamentous nitrogen-fixing cyanobacteria. *Planta* 228:617–625. <http://dx.doi.org/10.1007/s00425-008-0764-7>.
23. Zheng Y, Anderson S, Zhang Y, Garavito RM. 2011. The structure of sucrose synthase-1 from *Arabidopsis thaliana* and its functional implications. *J Biol Chem* 286:36108–36118. <http://dx.doi.org/10.1074/jbc.M111.275974>.
24. Lairson LL, Henrissat B, Davies GJ, Withers SG. 2008. Glycosyltransferases: structures, functions, and mechanisms. *Annu Rev Biochem* 77:521–555. <http://dx.doi.org/10.1146/annurev.biochem.76.061005.092322>.
25. Sheng F, Jia X, Yep A, Preiss J, Geiger JH. 2009. The crystal structures of the open and catalytically competent closed conformation of *Escherichia coli* glycogen synthase. *J Biol Chem* 284:17796–17807. <http://dx.doi.org/10.1074/jbc.M809804200>.
26. Hardin SC, Winter H, Huber SC. 2004. Phosphorylation of the amino terminus of maize sucrose synthase in relation to membrane association and enzyme activity. *Plant Physiol* 134:1427–1438. <http://dx.doi.org/10.1104/pp.103.036780>.
27. Klotz KL, Finger FL, Shelver WL. 2003. Characterization of two sucrose synthase isoforms in sugarbeet root. *Plant Physiol Biochem* 41:107–115. [http://dx.doi.org/10.1016/S0981-9428\(02\)00024-4](http://dx.doi.org/10.1016/S0981-9428(02)00024-4).
28. Schäfer WE, Rohwer JM, Botha FC. 2004. A kinetic study of sugarcane sucrose synthase. *Eur J Biochem* 271:3971–3977. <http://dx.doi.org/10.1111/j.1432-1033.2004.04288.x>.
29. Wolosiuk RA, Pontis HG. 1974. Studies on sucrose synthetase. Kinetic mechanism. *Arch Biochem Biophys* 165:140–145. [http://dx.doi.org/10.1016/0003-9861\(74\)90151-9](http://dx.doi.org/10.1016/0003-9861(74)90151-9).
30. Kuhn ML, Falaschetti CA, Ballicora MA. 2009. *Ostreococcus tauri* ADP-glucose pyrophosphorylase reveals alternative paths for the evolution of subunit roles. *J Biol Chem* 284:34092–34102. <http://dx.doi.org/10.1074/jbc.M109.037614>.
31. Sambrook J, Russell DW. 2001. Molecular cloning: a laboratory manual, 3rd ed, vol 2. Cold Spring Harbor Laboratory Press, Cold Spring Harbor, NY.
32. Laemmli UK. 1970. Cleavage of structural proteins during the assembly of the head of bacteriophage T4. *Nature* 227:680–685. <http://dx.doi.org/10.1038/227680a0>.
33. Hall TA. 1999. BioEdit: a user-friendly biological sequence alignment editor and analysis program for Windows 95/98/NT. *Nucleic Acids Symp Ser* 41:95–98.
34. Gouy M, Guindon S, Gascuel O. 2010. SeaView version 4: a multiplatform graphical user interface for sequence alignment and phylogenetic tree building. *Mol Biol Evol* 27:221–224. <http://dx.doi.org/10.1093/molbev/msp259>.
35. Winn MD, Ballard CC, Cowtan KD, Dodson EJ, Emsley P, Evans PR, Keegan RM, Krissinel EB, Leslie AG, McCoy A, McNicholas SJ, Murshudov GN, Pannu NS, Potterton EA, Powell HR, Read RJ, Vagin A, Wilson KS. 2011. Overview of the CCP4 suite and current developments. *Acta Crystallogr D Biol Crystallogr* 67:235–242. <http://dx.doi.org/10.1107/S0907444910045749>.
36. Diederichs K, Karplus PA. 2013. Better models by discarding data? *Acta Crystallogr D Biol Crystallogr* 69:1215–1222. <http://dx.doi.org/10.1107/S0907444913001121>.
37. McCoy AJ, Grosse-Kunstleve RW, Adams PD, Winn MD, Storoni LC, Read RJ. 2007. Phaser crystallographic software. *J Appl Crystallogr* 40:658–674. <http://dx.doi.org/10.1107/S0021889807021206>.
38. Emsley P, Cowtan K. 2004. Coot: model-building tools for molecular graphics. *Acta Crystallogr D Biol Crystallogr* 60:2126–2132. <http://dx.doi.org/10.1107/S0907444904019158>.
39. Murshudov GN, Vagin AA, Dodson EJ. 1997. Refinement of macromolecular structures by the maximum-likelihood method. *Acta Crystallogr D Biol Crystallogr* 53:240–255. <http://dx.doi.org/10.1107/S0907444996012255>.
40. Adams PD, Afonine PV, Bunkoczi G, Chen VB, Davis IW, Echols N, Headd JJ, Hung LW, Kapral GJ, Grosse-Kunstleve RW, McCoy AJ, Moriarty NW, Oeffner R, Read RJ, Richardson DC, Richardson JS, Terwilliger TC, Zwart PH. 2010. PHENIX: a comprehensive Python-based system for macromolecular structure solution. *Acta Crystallogr D Biol Crystallogr* 66:213–221. <http://dx.doi.org/10.1107/S0907444909052925>.
41. Sali A, Blundell TL. 1993. Comparative protein modelling by satisfaction of spatial restraints. *J Mol Biol* 234:779–815. <http://dx.doi.org/10.1006/jmbi.1993.1626>.
42. Lüthy R, Bowie JU, Eisenberg D. 1992. Assessment of protein models with three-dimensional profiles. *Nature* 356:83–85. <http://dx.doi.org/10.1038/356083a0>.
43. Richards FM, Kundrot CE. 1988. Identification of structural motifs from protein coordinate data: secondary structure and first-level supersecondary structure. *Proteins* 3:71–84. <http://dx.doi.org/10.1002/prot.340030202>.
44. Gibson RP, Tarling CA, Roberts S, Withers SG, Davies GJ. 2004. The donor subsite of trehalose-6-phosphate synthase: binary complexes with UDP-glucose and UDP-2-deoxy-2-fluoro-glucose at 2 Å resolution. *J Biol Chem* 279:1950–1955. <http://dx.doi.org/10.1074/jbc.M307643200>.
45. Duncan KA, Huber SC. 2007. Sucrose synthase oligomerization and F-actin association are regulated by sucrose concentration and phosphorylation. *Plant Cell Physiol* 48:1612–1623. <http://dx.doi.org/10.1093/pcp/pcm133>.
46. Guerrero-Barrera AL, Garcia-Cuellar CM, Villalba JD, Segura-Nieto M, Gomez-Lojero C, Reyes ME, Hernandez JM, Garcia RM, de la Garza M. 1996. Actin-related proteins in *Anabaena* spp. and *Escherichia coli*. *Microbiology* 142(Part 5):1133–1140.
47. Buschiazzo A, Ugalde JE, Guerin ME, Shepard W, Ugalde RA, Alzari PM. 2004. Crystal structure of glycogen synthase: homologous enzymes catalyze glycogen synthesis and degradation. *EMBO J* 23:3196–3205. <http://dx.doi.org/10.1038/sj.emboj.7600324>.
48. Yep A, Ballicora MA, Preiss J. 2006. The ADP-glucose binding site of the *Escherichia coli* glycogen synthase. *Arch Biochem Biophys* 453:188–196. <http://dx.doi.org/10.1016/j.abb.2006.07.003>.
49. Gibson RP, Turkenburg JP, Charnock SJ, Lloyd R, Davies GJ. 2002. Insights into trehalose synthesis provided by the structure of the retaining glycosyltransferase OtsA. *Chem Biol* 9:1337–1346. [http://dx.doi.org/10.1016/S1074-5521\(02\)00292-2](http://dx.doi.org/10.1016/S1074-5521(02)00292-2).
50. Schinzel R, Druceckes P. 1991. The phosphate recognition site of *Escherichia coli* maltodextrin phosphorylase. *FEBS Lett* 286:125–128. [http://dx.doi.org/10.1016/0014-5793\(91\)80956-4](http://dx.doi.org/10.1016/0014-5793(91)80956-4).
51. Schinzel R, Palm D. 1990. *Escherichia coli* maltodextrin phosphorylase: contribution of active site residues glutamate-637 and tyrosine-538 to the phosphorylytic cleavage of alpha-glucans. *Biochemistry* 29:9956–9962. <http://dx.doi.org/10.1021/bi00494a028>.
52. Yep A, Ballicora MA, Preiss J. 2004. The active site of the *Escherichia coli* glycogen synthase is similar to the active site of retaining GT-B glycosyltransferases. *Biochem Biophys Res Commun* 316:960–966. <http://dx.doi.org/10.1016/j.bbrc.2004.02.136>.
53. Lee SS, Hong SY, Errey JC, Izumi A, Davies GJ, Davis BG. 2011. Mechanistic evidence for a front-side, S_Ni-type reaction in a retaining glycosyltransferase. *Nat Chem Biol* 7:631–638. <http://dx.doi.org/10.1038/nchembio.628>.
54. Gomez H, Lluch JM, Masgrau L. 2013. Substrate-assisted and nucleophilically assisted catalysis in bovine alpha1,3-galactosyltransferase. Mechanistic implications for retaining glycosyltransferases. *J Am Chem Soc* 135:7053–7063.
55. Mitchell EP, Withers SG, Ermert P, Vasella AT, Garman EF, Oikonomakos NG, Johnson LN. 1996. Ternary complex crystal structures of glycogen phosphorylase with the transition state analogue nojirimycin tetrazole and phosphate in the T and R states. *Biochemistry* 35:7341–7355. <http://dx.doi.org/10.1021/bi960072w>.
56. Díaz A, Diaz-Lobo M, Grados E, Guinovart JJ, Fita I, Ferrer JC. 2012. Lyase activity of glycogen synthase: is an elimination/addition mechanism a possible reaction pathway for retaining glycosyltransferases? *IUBMB Life* 64:649–658. <http://dx.doi.org/10.1002/iub.1048>.
57. Koshland DE. 1958. Application of a theory of enzyme specificity to protein synthesis. *Proc Natl Acad Sci U S A* 44:98–104. <http://dx.doi.org/10.1073/pnas.44.2.98>.
58. Johnson KA. 2008. Role of induced fit in enzyme specificity: a molecular forward/reverse switch. *J Biol Chem* 283:26297–26301. <http://dx.doi.org/10.1074/jbc.R800034200>.
59. Fersht A. 1999. Structure and mechanism in protein science: a guide to enzyme catalysis and protein folding. W H Freeman, New York, NY.
60. Gómez H, Polyak I, Thiel W, Lluch JM, Masgrau L. 2012. Retaining glycosyltransferase mechanism studied by QM/MM methods: lipopolysaccharyl-alpha-1,4-galactosyltransferase C transfers alpha-galactose via an oxocarbenium ion-like transition state. *J Am Chem Soc* 134:4743–4752. <http://dx.doi.org/10.1021/ja210490f>.
61. Chua TK, Bujnicki JM, Tan TC, Huynh F, Patel BK, Sivaraman J. 2008. The structure of sucrose phosphate synthase from *Halothermothrix orenii*

- reveals its mechanism of action and binding mode. *Plant Cell* 20:1059–1072. <http://dx.doi.org/10.1105/tpc.107.051193>.
62. Zheng L, Zhou X, Zhang H, Ji X, Li L, Huang L, Bai L, Zhang H. 2012. Structural and functional analysis of validoxylamine A 7'-phosphate synthase ValL involved in validamycin A biosynthesis. *PLoS One* 7:e32033. <http://dx.doi.org/10.1371/journal.pone.0032033>.
63. Cavalier MC, Yim YS, Asamizu S, Neau D, Almabruk KH, Mahmud T, Lee YH. 2012. Mechanistic insights into validoxylamine A 7'-phosphate synthesis by VldE using the structure of the entire product complex. *PLoS One* 7:e44934. <http://dx.doi.org/10.1371/journal.pone.0044934>.
64. Kolman MA, Nishi CN, Perez-Cenci M, Salerno GL. 2015. Sucrose in cyanobacteria: from a salt-response molecule to play a key role in nitrogen fixation. *Life (Basel)* 5:102–126.